



# Visual pathways evaluation in Kearns Sayre syndrome: a diffusion tensor imaging study

Maria Camilla Rossi-Espagnet<sup>1,2</sup> · Martina Lucignani<sup>3</sup> · Luca Pasquini<sup>1,2</sup> · Antonio Napolitano<sup>3</sup> · Stefano Pro<sup>4</sup> · Andrea Romano<sup>2,5</sup> · Daria Diodato<sup>6</sup> · Diego Martinelli<sup>7</sup> · Daniela Longo<sup>1</sup>

Received: 25 June 2019 / Accepted: 4 October 2019 / Published online: 4 November 2019  
© Springer-Verlag GmbH Germany, part of Springer Nature 2019

## Abstract

**Purpose** Kearns Sayre syndrome (KSS) is a mitochondrial disorder characterized by development of visual impairment. Electroretinogram (ERG) and visual evoked potentials are not able to provide topographical information of optic damage. The purpose of this study was to explore retrochiasmatic optic pathway alteration in KSS with diffusion tractographic analysis and to compare it with different tracts.

**Methods** DTI from 8 KSS subjects (14.7 years) and 10 healthy controls (HC) were acquired on a 3T scanner. Optic radiations (OR), optic tracts (OT), inferior frontooccipital fasciculus (IFOF) and corticospinal tract (CST) were reconstructed with probabilistic tractography. Fractional anisotropy (FA), apparent diffusion coefficient (ADC), radial (RD), and axial diffusivity (AD) were calculated, evaluating group differences. *T* test on diffusion parameters identified significantly different track portions among cohorts.

**Results** All patients had optic pathway alterations at electrophysiological examination. Significant lower FA were found in OT, IFOF, and CST of KSS group. RD was significantly higher in bilateral OR, IFOF, CST, and right OT, while ADC was higher in bilateral OR and CST. RD values were higher in the proximal and distal portion of OR bilaterally and in the distal portion of right OT, while widespread differences were found in IFOF and CST. No significant differences were found for AD. FA profiles analysis demonstrated significant differences between groups in several regions of OT, IFOF, and CST, while ADC assessment revealed spread differences in OR and CST.

**Conclusions** DTI evaluation of retrochiasmatic tracks may represent a useful tool to topographically investigate retrochiasmatic visual impairment in KSS.

**Keywords** Kearns Sayre syndrome · Diffusion tensor imaging · Mitochondrial disorders · Optic pathway · Leukodystrophy

## Abbreviation

KSS Kearns Sayre syndrome  
ERG Electroretinogram

VEP Visual evoked potential  
FA Fractional anisotropy  
ADC Apparent diffusion coefficient

---

MCR-E and ML contributed equally to this work.

---

✉ Maria Camilla Rossi-Espagnet  
mcamilla.rossi@opbg.net

<sup>1</sup> Neuroradiology Unit, Imaging Department, Bambino Gesù Children's Hospital, IRCCS, Piazza Sant'Onofrio 4, 00100 Rome, Italy

<sup>2</sup> NESMOS Department, Sant'Andrea Hospital, Sapienza University, Rome, Italy

<sup>3</sup> Medical Physics Department, Bambino Gesù Children's Hospital, IRCCS, Rome, Italy

<sup>4</sup> Neurology Unity, Department of Neurosciences, Bambino Gesù Children's Hospital, IRCCS, Rome, Italy

<sup>5</sup> Department of Odontostomatological and Maxillo-Facial Sciences, Umberto I Hospital, Sapienza University, Rome, Italy

<sup>6</sup> Unit of Neuromuscular and Neurodegenerative Disorders, Laboratory of Molecular Medicine, Bambino Gesù Children's Hospital, IRCCS, Rome, Italy

<sup>7</sup> Division of Metabolism and Research Unit of Metabolic Biochemistry, Bambino Gesù Children's Hospital, IRCCS, Rome, Italy

RD	Radial diffusivity
AD	Axial diffusivity
HC	Healthy controls
PR-VEP	Pattern reversal visual evoked potential
OR	Optic radiation
OT	Optic tract
IFOF	Inferior frontooccipital fasciculus
CST	Corticospinal tract
FOD	Fiber orientation distribution
GA	Global average
LA	Local average
PEO	Progressive external ophthalmoplegia

## Introduction

Kearns Sayre syndrome (KSS) is a rare genetic disorder characterized by the classical clinical triad of chronic progressive external ophthalmoplegia, retinal pigmentary degeneration, and cardiac conduction block [1].

The clinical onset of the disorder is before the age of 20 years after an initial normal development with a variety of symptoms including ataxia, myopathy, endocrine disturbances, and hearing loss. The diagnosis of the disease is suspected by integration of clinical, laboratory, and imaging findings. The final diagnostic confirmation requires muscle biopsy and genetic demonstration of a heteroplasmic deletion, or less frequently duplication, of mitochondrial DNA [2]. In about one-third of the patients a common deletion of mitochondrial DNA of 4977 bp is reported [3].

Conventional MR imaging initially demonstrates subtle signal alteration of pontine and midbrain tegmentum with progressive involvement of basal ganglia and bi-hemispheric infra- and supratentorial white matter (WM). U-fibers are predominantly involved while periventricular WM is usually spared [4, 5].

Visual impairment with progressive external ophthalmoplegia and pigmentary retinal degeneration affect KSS patients since the initial stage of the disease [6, 7]. Electrophysiological methods such as electroretinogram (ERG) and visual evoked potentials (VEP) may provide important functional information but are not able to topographically assess damage localization along the WM pathway [6]. ERG provides a basis to establish the diagnosis of widespread progressive forms of retinitis pigmentosa in early life even when visible fundus abnormalities at ophthalmoscope examination are minimal or absent, while VEP alterations suggest retroretinal visual pathway involvement [8, 9].

Moreover, contrary to other mitochondrial disorders such as Leber's hereditary optic neuropathy and cone-rod dystrophy, in KSS leukodystrophy may represent an additional factor that could contribute to visual pathway damage, despite

optic tracts (OT), and optic radiations (OR) are mainly spared on conventional MRI [10].

DTI is an advanced MR technique that allows quantification of water diffusion in terms of anisotropic or isotropic movement, as expressed by the fractional anisotropy (FA) parameter that provides information about the anisotropic structure of the brain [10]. Along with FA, myelination and axonal damage can be further explored by investigating DTI specific eigenvectors, thus characterizing axial (AD) and radial (RD) water diffusivity within the main axonal tracts [11]. DTI with tractographic reconstruction has the additional advantage to allow reconstruction of a specific WM tract, providing structural information on functional pathways such as the visual system [12]. In the last 10 years, the use of diffusion techniques has spread out in the investigation of many brain disorders, and only recently, they were applied to study metabolic disorders. The aims were mainly two: to contribute to the exploration of pathophysiologic mechanisms underlying a specific functional impairment and to provide early information about clinical outcome [13].

The purpose of this study was to explore retrochiasmatic optic pathway microstructural alterations in a group of patients affected by KSS by means of DTI tractographic analysis, including topographical evaluation of DTI parameters modifications within the length of the tracts. The same analysis was also applied on two different tracts such as the inferior frontooccipital fasciculus (IFOF) and the corticospinal tract (CST) in order to compare the profiles of DTI parameters modifications with those of the retrochiasmatic optic pathway.

## Methods

### Subjects

This research was conducted in accordance with the Declaration of Helsinki. Ethical committee approval was obtained through Research approval was obtained through the ethical committee of Bambino Gesù Children's Hospital (protocol number 1867/2019) and written informed consent was obtained from every subject or next of kin for the execution of the MR exams.

Between 2016 and 2018, the MRIs from all patients affected by KSS followed in our institution were retrospectively evaluated.

The patients were enrolled in the study if fulfilling the following inclusion criteria: (a) genetic diagnosis of KSS; (b) presence of a MRI study with non-artifacted DTI acquisition; (c) electrophysiological evaluation with ERG and VEP.

Additionally, a group of age-matched healthy controls (HC) with no neurologic or psychiatric disorder and unremarkable MRI including a DTI sequence was included in the study.

## Electrophysiological evaluation: electroretinogram and visual evoked potential

All patients had an electrophysiological evaluation in order to assess retinal and optic pathway functional damage respectively recording ERG and VEP.

ERG was detected by conventional silver–silver chloride cup electrodes attached to the lower eyelid and referred to Fz, with the ground on the ear lobe. The stimulation rate of the bright white was 1.2 Hz. The analysis time for ERG recording was 500 ms and the bandpass 1–250 Hz. Between 50 and 100 responses were averaged and repeated at least twice. We evaluated ERG response as normal or absent.

Flash-visual evoked potentials (Flash-VEP) were recorded separately for each eye, through silver-silver chloride cup electrodes placed over O<sub>2</sub>-Oz-O<sub>1</sub> and Cz with ground on the ear lobe. The stimulation rate of the bright white was 1.2 Hz. The analysis time for Flash-VEP recording was 500 ms and the bandpass 1–250 Hz. Between 50 and 100 responses were averaged and repeated at least twice. We evaluated Flash-VEP response as normal, with increase latency of P2 or absent.

The pattern reversal-visual evoked potentials (PR-VEP) were recorded separately for each eye, through silver–silver chloride cup electrodes placed over O<sub>2</sub>-Oz-O<sub>1</sub> and Cz with ground on the ear lobe. Black and white checkerboard patterns with a spatial frequency of 2 c/deg (30 min of arc for each check) with a level of luminance of 50 cd/m<sup>2</sup> and contrast 400/1 were delivered monocularly. The analysis time for PR-PEV recording was 500 ms and the bandpass 2–200 Hz. Pattern stimuli were reversed twice a second with a variability of ± 10% randomly. Between 50 and 100 responses were averaged and repeated at least twice. We evaluated Flash-VEP response as normal, with increase latency of P100 or absent.

For PR-VEP each subject was asked to fix the screen center and identify a specific bright spot. PR-VEP was recorded in all patients except in one of them showing flash-VEP absence. Flash-VEP, in clinical practice, is usually preferred in patients without the ability to maintain visual attention. In our case series, we did not perform Flash-VEP in two patients.

## MR imaging acquisition and evaluation

Images from both cohorts were acquired on a 3T Siemens Magnetom Skyra scanner (Siemens Medical Systems, Erlangen, Germany) equipped with 32 channels head-coil.

Brain MRI protocol consisted of: axial spin echo T2-weighted sequences sequences (TR 8600 ms, TE 122 ms, ST 3 mm), coronal turbo spin echo T2-weighted sequence (TR 6380 ms, TE 108 ms, ST 3 mm), axial FLAIR sequences (TR 9000 ms, TE: 2500 ms, TI 85 ms, ST 3 mm), sagittal 3D-MPRAGE sequence (TR 2060 ms, TE 1040 ms, TI 2.26 ms, ST 0.8 mm), and axial DTI sequence (TR 8300 ms, TE 99 ms, ST 2 mm). For DTI sequence, three DWI shells were

acquired: (1) 10 averages with  $b = 0$  s/mm<sup>2</sup>, (2)  $b = 1000$  s/mm<sup>2</sup>, and (3)  $b = 1500$  s/mm<sup>2</sup>, both with gradients along 30 directions. Images had a spatial resolution of  $2.0 \times 2.0 \times 2.0$  mm, acquisition matrix =  $896 \times 896$ .

Brain MR images were evaluated in consensus by two pediatric neuroradiologists with 4 and 20 years of experience.

## DTI data processing

DTI data were processed using MRtrix3 (<https://github.com/mrtrix3>). Data were denoised via PCA algorithm (dwidenoise) and corrected for distortion due to eddy currents via ACID toolbox (<http://www.diffusiontools.com/>). The maps were attained by exploiting “dwi2mask” for brain masking, “dwi2tensor” for tensor fitting and “tensor2metric” to compute FA, AD, RD, and ADC maps.

We identified OR, OT, IFOF, and CST using constrained spherical deconvolution (CSD) approach as provided in MRtrix3 (Tournier et al. 2012). To perform automatic tracking and minimize manual inputs, different regions of interest (ROIs) were manually drawn on the high-resolution anatomical template (<https://github.com/Chaogan-Yan/REST>). OR and OT were generated locating ROIs at the optic chiasm (OC), lateral geniculate nucleus (LGN), and occipital cortex (V3), while IFOF was reconstructed between ventral occipital lobe (VOL) and orbitofrontal cortex (OFC). Finally, CST was generated between precentral gyrus (PG) and anterior medullary area (AMA).

The non-diffusion-weighted ( $b = 0$ ) images were registered (warping) to the common template via the greedy symmetric diffeomorphic normalization algorithm of the advanced normalization tools (<https://github.com/ANTsX>). Then, inverse warping was used to back-projected the ROIs on the b0 image and then WM tracts were reconstructed in each individual’s native space based upon warped ROIs.

CSD streamlines algorithm allowed fiber tracking to be performed (tckgen), computing the pathways between a pair of ROIs. To reduce the algorithm dependence on starting seeding ROI, tracks between a pair of ROIs were generated as two different fiber paths: one forward path (from ROI1 to ROI2) and one backward path (from ROI2 to ROI1). Criteria for track termination included maximum number of streamlines (200000), threshold on the anisotropy of diffusion tensor (0.1 by default) and maximum angle between successive steps (40°). We further refined tracks (tckedit) specifying exclusion ROI and thus reducing the number of fiber pathways.

Matlab (version R2017a) was then used to create a unique fiber streamline by merging tracks from forward to backward paths. To clean each fiber group into a compact bundle, fibers extending beyond the position of the target ROI were cut in proximity of ROI centroid and fibers that are more than 150% above the mean fiber length were removed.

Global average (GA) measurements were obtained within tracks for each diffusion tensor parameter. Moreover, for those DTI parameters providing statistically significant difference between groups in the GA, a local average (LA) profile was also computed in Matlab. To this purpose, we first interpolated each fiber to have the same number of points (i.e., 100), and then we assessed diffusion parameter values on each point along the fiber.

## Statistical analysis

For electrophysiological evaluation percentage and range were calculated in the patients group for descriptive purposes.

Mean and standard deviation (SD) of the diffusion tensor parameters were computed for KSS subjects and HC. We assessed group differences within each track by using a two sample *T* test. Similarly, *T* test was also performed on LA diffusion tensor parameters profiles in order to identify the portion of track with the highest significant difference between the two groups. All statistical analyses were performed with MATLAB software (version R2017a) with significance set at 0.05.

## Results

### Patients

Between January 2016 and December 2018, a total of 11 patients with a genetically confirmed diagnosis of KSS underwent MR examination as part of their diagnostic work-up or follow-up. Of them, 3 DTI images were not acquired for lack of cooperation and the patients were not included in the study. A group of 8 subjects (4 female and 4 male, mean age =  $14.7 \pm 3.7$  years) fulfilled the inclusion criteria and was retrospectively included in the study.

All patients had a deletion of mitochondrial DNA ranging from 5000 to 8000 bp.

Additionally, a group of 10 age-matched HC was included (4 females, 6 males, mean age =  $14.6 \pm 4.7$  years).

### Electrophysiological findings

ERG was absent in 6/8 patients and normal in 2/8 patients. Flash VEP had normal latency and reduced amplitude in 2/8 patients, increased latency of P2 and reduced amplitude in 3/8 patients and they were not performed in 2/8 patients. PR-VEP were absent in 3/8 patients, abnormal with increase latency of P100 in 4/8 patients and not performed in 1/8 patients.

All patient's demographic data and electrophysiological findings are summarized in Table 1.

## Conventional MR imaging findings in KSS

A summary of typical WM and GM involvement on conventional MRI is depicted in Fig. 1. All our patients showed bilateral and symmetrical involvement of the cerebellar WM (8/8) and superior cerebellar peduncles (8/8), with variable extension to the middle cerebellar peduncles (6/8). Brainstem abnormalities were present in all patients (8/8). The brainstem T2 hyperintensity tended to spare the red nuclei, with variable involvement of the substantia nigra (6/8). The diencephalon was compromised in all the patients, predominantly at the level of the hypothalamus (8/8), extending to the thalami in 6/8. The basal ganglia were involved in 6/8 patients, predominantly at the level of the globus pallidus. The supratentorial subcortical WM was involved in five patients, while in the remaining three patients, it was minimally abnormal. Periventricular WM, including OR, was spared in all patients. OT were also lacking of visible signal alteration, demonstrating slight thinning in four patients with mild generalized cerebral and cerebellar atrophy.

### DTI

Tractographic reconstruction of bilateral OR, OT, IFOF, and CST was performed in all patients and controls. *T* test analysis demonstrated a statistically significant difference in GA for FA values in bilateral OT, IFOF, and CST with lower values in the KSS group. RD values were significantly higher in KSS group compared with HC in OR, IFOF, and CST bilaterally and in the right OT, whereas ADC values were also significantly higher in KSS group in OR and CST bilaterally (Table 2). No significant differences were obtained between KSS group and HC in GA for AD values comparison.

The evaluation of LA for FA values demonstrated significant differences between groups in several regions of OT ( $p < 0.02$ ), IFOF ( $p < 0.03$ ), and CST ( $p < 0.01$ ). ADC assessment on OR showed higher KSS values widespread along the tract ( $p < 0.03$ ), while ADC on CST revealed asymmetric behavior, with spread differences in the left portion ( $p < 0.02$ ) and no differences in the right.

Comparison of LA for RD values revealed higher difference in the proximal and distal portion of the OR bilaterally ( $p < 0.01$ ) and the distal portion of the right OT ( $p < 0.02$ ) (Fig. 2). Finally, LA evaluation of RD values showed significant differences between KSS and HC in several regions along bilateral CST ( $p < 0.02$ ) and IFOF ( $p < 0.02$ ) (Fig. 3).

## Discussion

Patients with KSS are consistently affected by ptosis, progressive external ophthalmoplegia (PEO), optic atrophy, and/or retinal dystrophy [6].



**Table 1** Demographic and electrophysiological data from the patient group

ID	Sex	AGE at diagnosis (years)	AGE at last MR (years)	ERG	Flash-VEP P2 latency (ms)	Flash-VEP N1-P2 amplitude ( $\mu$ V)	PR-VEP P100 latency (ms)	PR-VEP N75-P100 amplitude ( $\mu$ V)
1	M	8	11	Absent	Normal	8.29	Absent	Absent
2	F	8	14	Absent	150	6.68	175	4.53
3	M	8	12	Absent	130	9.63	136	8.37
4	F	13	19	Absent	Normal	11.52	133	8.10
5	F	12	13	Absent	135	4.58	Absent	Absent
6	F	9	11	Absent	Absent	Absent	Not performed	Not performed
7	M	14	16	Normal	Not performed	Not performed	130	7.63
8	M	13	22	Normal	Not performed	Not performed	Absent	Absent

Normal reference value for P2 latency  $105 \pm 8$  ms (mean  $\pm$  standard deviation); normal reference value for P100 latency  $108 \pm 11$  ms (mean  $\pm$  standard deviation). Normal reference value for N1-P2 amplitude  $27 \pm 11$   $\mu$ V; normal reference for N75-P100 amplitude was  $4.10 \pm 2.20$   $\mu$ V

The large density of mitochondria found in optic nerve head along with the high photoreceptor cells energy requirements are considered as the main factors that contribute to visual impairment in KSS, as well as other primary mitochondrial disorders such as Leber optic neuropathy and cone-rod dystrophy [6, 14].

Neurophysiologic examination with ERG is considered of great utility in demonstrating rod cells impairment, revealing the entity of retinal involvement in visual disturbances [15]. VEP may also contribute to the investigation of visual impairment, revealing reduced potential amplitude and increased

latency as the result of optic pathway damage. In our population, ERG response was absent in 6/8 KSS affected patients, and VEP were variably altered in all subjects in agreement with the diagnosis and the interval time from disease onset. However, the results obtained by electrophysiological tests are not able to provide topographical information about optic pathway damage, and specifically to explore the physiopathologic contribution of leukodystrophy to its impairment.

In non-syndromic mitochondrial disorders such as Leber's hereditary optic neuropathy and cone-rod dystrophy cerebral WM is unremarkable on conventional MRI but the application

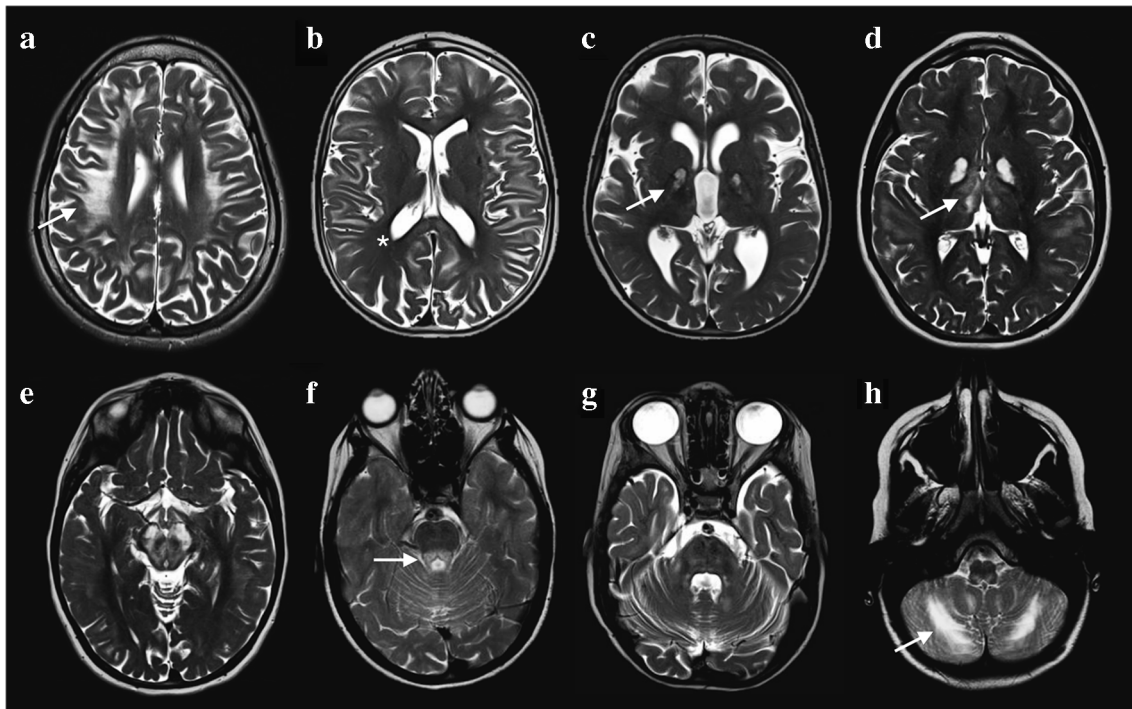


**Fig. 1** Typical MR findings in Kearns Sayre syndrome. Axial T2-weighted images from different patients (a-h) depict the characteristic radiologic features of the disease in the brain: subcortical white matter involvement with periventricular sparing (a white arrow; b asterisk);

bilateral signal alterations in the globus pallidus (c white arrow) thalami and hypothalami (d white arrow); brainstem involvement with predominant signal abnormalities in the tegmentum (f white arrow; g); cerebellar white matter (h white arrow)

**Table 2** Diffusion parameter values in optic radiation, optic tract, inferior frontooccipital fasciculus (IFOF) and corticospinal tract (CST). Unit of RD ADC is  $\mu\text{m}^2/\text{s}$ 

	Mean $\pm$ SD FA values		Mean $\pm$ SD RD values ( $\times 10^{-4}$ )		Mean $\pm$ SD ADC values ( $\times 10^{-4}$ )	
	HC	KSS ( <i>p</i> value)	HC	KSS ( <i>p</i> value)	HC	KSS ( <i>p</i> value)
Optic radiation right	0.47 $\pm$ 0.09	0.46 $\pm$ 0.04 (0.7811)	5.59 $\pm$ 0.59	6.50 $\pm$ 0.74 (0.0106)	7.89 $\pm$ 0.25	8.86 $\pm$ 0.875 (0.0039)
Optic radiation left	0.47 $\pm$ 0.11	0.45 $\pm$ 0.04 (0.5744)	5.85 $\pm$ 0.69	7.04 $\pm$ 1.16 (0.0159)	8.19 $\pm$ 0.26	9.36 $\pm$ 1.29 (0.0125)
Optic tract right	0.39 $\pm$ 0.05	0.31 $\pm$ 0.03 (0.0016)	8.02 $\pm$ 0.86	10 $\pm$ 2.72 (0.0425)	10 $\pm$ 0.85	12 $\pm$ 2.87 (0.1098)
Optic tract left	0.40 $\pm$ 0.05	0.30 $\pm$ 0.04 (0.0002)	7.86 $\pm$ 0.71	9.87 $\pm$ 3.07 (0.0596)	10 $\pm$ 0.67	12 $\pm$ 3.26 (0.1763)
IFOF right	0.35 $\pm$ 0.01	0.29 $\pm$ 0.00 (5.7e-4)	6.73 $\pm$ 0.14	7.63 $\pm$ 0.25 (0.0070)	8.31 $\pm$ 0.13	8.97 $\pm$ 0.28 (0.0504)
IFOF left	0.34 $\pm$ 0.01	0.30 $\pm$ 0.00 (0.0152)	6.84 $\pm$ 0.16	7.60 $\pm$ 0.20 (0.0117)	8.41 $\pm$ 0.12	8.99 $\pm$ 0.24 (0.0488)
CST right	0.43 $\pm$ 0.01	0.33 $\pm$ 0.01 (9.7e-8)	5.82 $\pm$ 0.15	8.04 $\pm$ 0.64 (0.003)	7.75 $\pm$ 0.14	9.58 $\pm$ 0.67 (0.0124)
CST left	0.42 $\pm$ 0.00	0.34 $\pm$ 0.01 (5.4e-7)	5.79 $\pm$ 0.19	7.77 $\pm$ 0.28 (2.2e-5)	7.69 $\pm$ 0.18	9.33 $\pm$ 0.31 (2.9e-4)

of DTI tractography for retrochiasmatic optic pathway evaluation has demonstrated microstructural WM alterations, suggesting an anterograde trans-synaptic degeneration [10].

Trans-synaptic degeneration refers to the disruption of neurons and axons following injury to cells with which they synapse. As a consequence of retinal damage, trans-synaptic

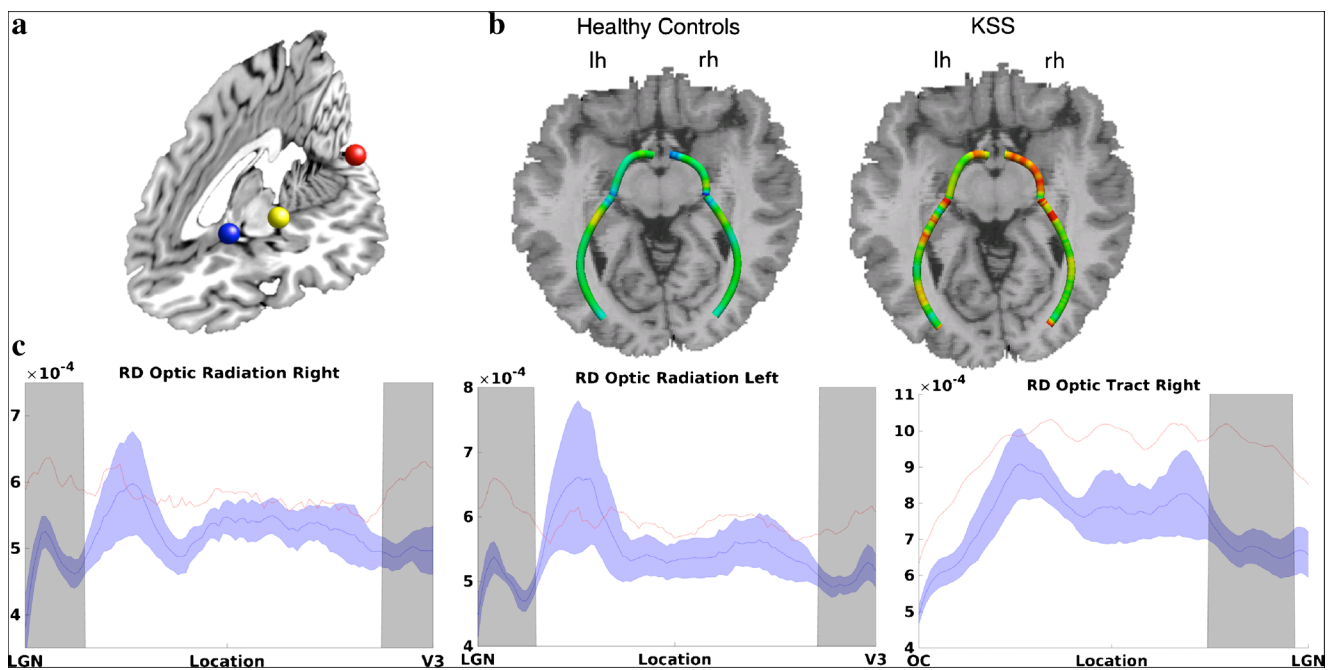


**Fig. 2** Analysis of radial diffusivity profile along optic radiations and optic tracts. **a** Schematic representation of the ROIs respectively located in optic chiasm (OC, blue), lateral geniculate nucleus (LGN, yellow) and occipital cortex (V3, red). **b** Mean radial diffusivity (RD) values displayed on bilateral optic radiations (OR) and optic tracts (OT) surfaces for healthy controls and Kearns Sayre syndrome (KSS) patients. **c** Mean RD profiles along right OR (left), left OR (middle) and right OT (right),

evaluated in the anterior-posterior direction. KSS patient values (red) were compared with the distribution of healthy controls (HC, blue). The lighter blue shades show range of  $\pm$  standard deviation from the HC mean. Shaded grey regions indicate the portions of tracts showing a significant main effect of KSS group RD values (*t* test, *p* < 0.05). Unit of RD is  $\mu\text{m}^2/\text{s}$

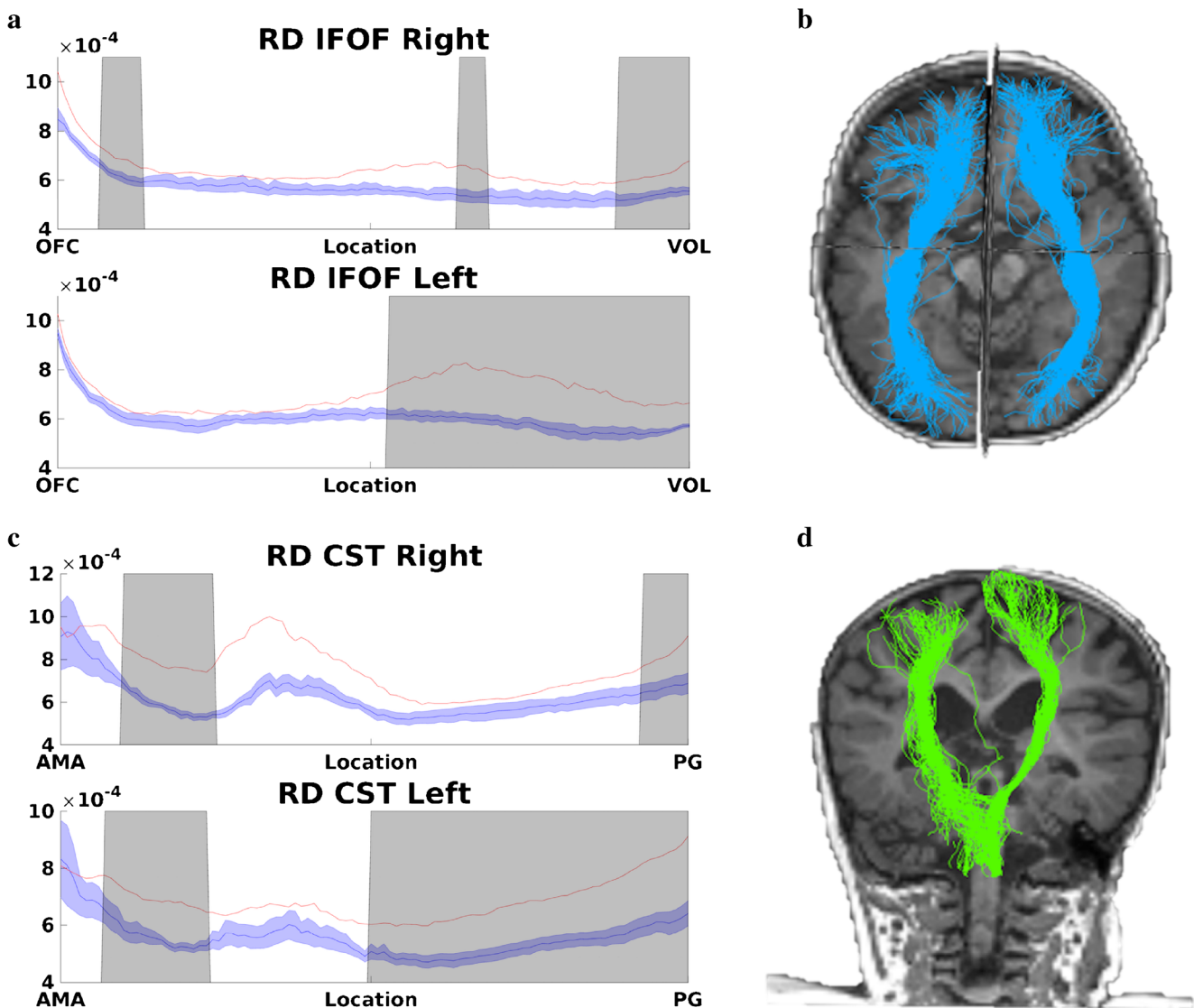


**Fig. 3** Analysis of radial diffusivity profile along inferior frontooccipital fasciculus and cortico-spinal tracts. **a** Mean RD profiles along right and left inferior frontooccipital fasciculus (IFOF) evaluated in the anterior–posterior direction from the orbitofrontal cortex (OFC) to the ventral occipital lobe (VOL) and **b** IFOF 3D rendering. **c** Mean RD profiles along right and left corticospinal tract (CST), evaluated in the caudocranial direction from the anterior medullary area (AMA) and

precentral gyrus (PG) and **d** CST 3D rendering. KSS patient values (red) were compared with the distribution of healthy controls (HC, blue). The lighter blue shades show range of  $\pm$  standard deviation from the HC mean. Shaded grey regions indicate the portions of tracts showing a significant main effect of KSS group RD values ( $t$  test,  $p < 0.05$ ). Unit of RD is  $\mu\text{m}^2/\text{s}$  (**a**, **c**)

degeneration may occur in mitochondrial optic neuropathies involving postsynaptic neurons (anterograde) of the retrochiasmatic tracts [16].

The specific etiology of the retrochiasmatic optic pathway impairment in KSS is currently unknown, but two main mechanisms may be hypothesized: an indirect mechanism due to retinopathy via trans-synaptic degeneration and a direct one caused by the leukodystrophy.

KSS remains unclassified in the most recent classification of brain leukodystrophies [17], being the pathologic processes involving the brain cells of these patients still poorly defined. However, similarly to the majority of mitochondrial

leukodystrophies, in KSS both white and gray matter are involved. The hemispheric WM impairment is mainly subcortical, including the U-fibers with sparing of the periventricular regions, similarly to other mitochondrial encephalopathies such as L-2-hydroxyglutaric aciduria [18].

Given the subcortical WM involvement and prevalent apparent sparing of periventricular WM, we aimed to investigate whether DTI parameters along retrochiasmatic optic pathway could demonstrate microstructural alterations in KSS compared with HC.

Our results demonstrate a significant difference in FA and ADC values between KSS patients and HC. The KSS group

demonstrated reduced FA in both OT and increased ADC values in OR suggesting disorganization in axon fibers of these tracts. These results were in line with the electrophysiological data demonstrating an impaired conduction along visual pathway in the majority of patients. Moreover, we found a significant difference in RD with increased values in OR and in the right OT of KSS patients compared with HC and without significant differences in AD between the two groups. Moreover, RD was also significantly increased in KSS patients in other WM tracts such as the IFOF and CST, confirming a diffuse alteration of the supra and infratentorial WM in the disorder.

RD is interpreted as a “biomarker” of myelin status. As suggested from animal studies and studies on multiple sclerosis with radiological–pathological correlation, high values may indicate increased astrogliosis and demyelination [19–21].

Human and animal studies in progressive demyelinating disease, such as multiple sclerosis, demonstrated a statistically significant correlation between VEP and DTI parameters, with stronger correlation with RD compared with other parameters, thus suggesting its potential role in reflecting microstructural alterations underlying the functional impairment [22, 23].

Similarly to the study of Ogawa et al. we also aimed to specifically investigate DTI parameters along the WM tracts profiles (LA) in order to topographically explore microstructural alterations along the retrochiasmatic visual pathway and to speculate potential physiopathological mechanisms underlying diffusion abnormalities [10]. This analysis demonstrated that significant differences of both FA and ADC values in OT and OR where localized along the tracts but RD differences especially in OR were mainly localized in the proximal and distal portion of the tracts, namely the lateral geniculate nucleus and the subcortical occipital WM. From these results, we may speculate that, together with the well-known retinal and optic nerve degeneration in patients affected by KSS, the presence of leukodystrophy may contribute to retrochiasmatic optic pathway alteration as expressed by the topographically defined alterations of RD [10, 16, 24]. On the other hand, WM tracts with a different course such as the IFOF and the CST exhibit more extensive alterations of DTI parameters along the tracts. This reflects their anatomical relations with the extension of leukodystrophy compared with the more spared periventricular regions.

The role of demyelination in this disorder has been recently pathologically proven in a post-mortem study that has demonstrated a predominant loss of myelin-associated glycoprotein in oligodendrocytes of patients affected by KSS, thus suggesting a possible distal dying-back oligodendroglialopathy [25].

Main limitations of our work are represented by the inclusion of patients with advanced disease (mean duration between diagnosis and MRI was 3.8 years) that prevented the possibility to use DTI parameters as an early “biomarkers” of

microstructural damage. Moreover, we do not have a follow-up of the patients, and we cannot speculate the potentiality of DTI parameters, and especially RD, as possible predictors of clinical outcome. An evaluation of pre-chiasmatic pathways was not performed in the present study due to the spatial resolution of the DTI sequence ( $2 \times 2 \times 2$  mm) and the coexistence of optic atrophy. Finally, the relatively small sample included and its retrospective nature limited a possible statistical correlation between ERG, VEP latency, and amplitude data and DTI parameters. Future studies should be addressed to investigate DTI parameters alterations along optic pathway in the early stage of the disorder, especially before occurrence of supratentorial WM alterations. Such studies might be helpful to investigate about physiopathological mechanisms underlying visual impairment in KSS and the usefulness of DTI parameters as an early imaging biomarker of this symptom.

## Conclusions

The results of this study suggest that DTI evaluation of retrochiasmatic optic pathway may provide a useful and complementary tool, together with electrophysiological data, to functionally and topographically investigate visual impairment in KSS, a primary mitochondrial disorder with leukodystrophy.

**Funding information** None.

## Compliance with ethical standards

**Conflict of interest** The authors declare that they have no conflict of interest.

**Ethical approval** All procedures performed in studies involving human participants were in accordance with the ethical standards of the institutional research committee and with the 1964 Helsinki declaration and its later amendments or comparable ethical standards.

**Informed consent** For this type of study, formal consent is not required.

## References

1. Kearns TP, Sayre GP (1958) Retinitis pigmentosa, external ophthalmoplegia, and complete heart block: unusual syndrome with histologic study in one of two cases. *AMA Arch Ophthalmol* 60:280–289. <https://doi.org/10.1001/archophth.1958.00940080296016>
2. Yamashita S, Nishino I, Nonaka I, Goto Y-I (2008) Genotype and phenotype analyses in 136 patients with single large-scale mitochondrial DNA deletions. *J Hum Genet* 53:598–606. <https://doi.org/10.1007/s10038-008-0289-8>



3. Davis R, Sue C (2011) The genetics of mitochondrial disease. *Semin Neurol* 31:519–530. <https://doi.org/10.1055/s-0031-1299790>
4. Hourani RG, Barada WM, Al-Kutoubi AM, Hourani MH (2006) Atypical MRI findings in Kearns-Sayre syndrome: T2 radial stripes. *Neuropediatrics* 37(2):110–113. <https://doi.org/10.1055/s-2006-924226>
5. Van der Knaap M, Valk J (2005) Myelination and myelin disorders, 3rd edn. Springer, New York, pp 231–220
6. Grönlund MA, Seyedi Honarvar AK, Andersson S et al (2010) Ophthalmological findings in children and young adults with genetically verified mitochondrial disease. *Br J Ophthalmol* 94(1):121–127. <https://doi.org/10.1136/bjo.2008.154187>
7. Yu M, Zhang Z, Wang QQ et al (2016) Clinical and brain magnetic resonance imaging features in a cohort of Chinese patients with Kearns-Sayre syndrome. *Chin Med J (Engl)* 129(12):1419–1424. <https://doi.org/10.4103/0366-6999.183417>
8. Scaiola V, Antozzi C, Villani F et al (1998) Utility of multimodal evoked potential study and electroencephalography in mitochondrial encephalomyopathy. *Ital J Neurol Sci* 19(5):291–300
9. Berson EL (1987) Electroretinographic findings in retinitis pigmentosa. *Jpn J Ophthalmol* 31(3):327–348
10. Ogawa S, Takemura H, Horiguchi H et al (2014) White matter consequences of retinal receptor and ganglion cell damage. *Invest Ophthalmol Vis Sci* 55(10):6976–6986. <https://doi.org/10.1167/iovs.14-14737>
11. Hofling AA, Kim JH, Fantz CR et al (2009) Diffusion tensor imaging detects axonal injury and demyelination in the spinal cord and cranial nerves of a murine model of globoid cell leukodystrophy. *NMR Biomed* 22(10):1100–1106. <https://doi.org/10.1002/nbm.1420>
12. Hofer S (2010) Reconstruction and dissection of the entire human visual pathway using diffusion tensor MRI. *Front Neuroanat* 4:15. <https://doi.org/10.3389/fnana.2010.00015>
13. Poretti A, Meoded A, Fatemi A (2016) Diffusion tensor imaging: a biomarker of outcome in Krabbe's disease. *J Neurosci Res* 94(11):1108–1115. <https://doi.org/10.1002/jnr.23769>
14. Barron MJ (2004) The distributions of mitochondria and sodium channels reflect the specific energy requirements and conduction properties of the human optic nerve head. *Br J Ophthalmol* 88(2):286–290. <https://doi.org/10.1136/bjo.2003.027664>
15. Cooper LL, Hansen RM, Darras BT et al (2002) Rod photoreceptor function in children with mitochondrial disorders. *Arch Ophthalmol* 120(8):1055–1062
16. Manners DN, Rizzo G, La Morgia C et al (2015) Diffusion tensor imaging mapping of brain white matter pathology in mitochondrial optic neuropathies. *Am J Neuroradiol* 36:1259–1265. <https://doi.org/10.3174/ajnr.A4272>
17. van der Knaap MS, Bugiani M (2017) Leukodystrophies: a proposed classification system based on pathological changes and pathogenetic mechanisms. *Acta Neuropathol* 134:351–382. <https://doi.org/10.1007/s00401-017-1739-1>
18. Yang E, Prabhu SP (2014) Imaging manifestations of the leukodystrophies, inherited disorders of white matter. *Radiol Clin N Am* 52:279–319. <https://doi.org/10.1016/j.rcl.2013.11.008>
19. Song S-K, Sun S-W, Ramsbottom MJ, Chang C, Russell J, Cross AH (2002) Dysmyelination revealed through MRI as increased radial (but unchanged axial) diffusion of water. *Neuroimage* 17:1429–1436. <https://doi.org/10.1006/nimg.2002.1267>
20. Aung WY, Mar S, Benzinger TL (2013) Diffusion tensor MRI as a biomarker in axonal and myelin damage. *Imaging Med* 5:427–440. <https://doi.org/10.2217/iim.13.49>
21. Schmierer K, Wheeler-Kingshott CAM, Tozer DJ, Boulby PA, Parkes HG, Yousry TA, Scaravilli F, Barker GJ, Tofts PS, Miller DH (2008) Quantitative magnetic resonance of postmortem multiple sclerosis brain before and after fixation. *Magn Reson Med* 59:268–277. <https://doi.org/10.1002/mrm.21487>
22. Naismith RT, Xu J, Tutlam NT, Trinkaus K, Cross AH, Song SK (2010) Radial diffusivity in remote optic neuritis discriminates visual outcomes. *Neurology* 74:1702–1710. <https://doi.org/10.1212/WNL.0b013e3181e0434d>
23. Nishioka C, Liang H-F, Chung C-F, Sun S-W (2017) Disease stage-dependent relationship between diffusion tensor imaging and electrophysiology of the visual system in a murine model of multiple sclerosis. *Neuroradiology* 59:1241–1250. <https://doi.org/10.1007/s00234-017-1904-1>
24. Milesi J, Rocca MA, Bianchi-Marzoli S, Petrolini M, Pagani E, Falini A, Comi G, Filippi M (2012) Patterns of white matter diffusivity abnormalities in Leber's hereditary optic neuropathy: a tract-based spatial statistics study. *J Neurol* 259:1801–1807. <https://doi.org/10.1007/s00415-011-6406-1>
25. Lax NZ, Campbell GR, Reeve AK, Ohno N, Zamboni J, Blakely EL, Taylor RW, Bonilla E, Tanji K, DiMauro S, Jaros E, Lassmann H, Turnbull DM, Mahad DJ (2012) Loss of myelin-associated glycoprotein in kearns-sayre syndrome. *Arch Neurol* 69:490–499. <https://doi.org/10.1001/archneurol.2011.2167>

**Publisher's note** Springer Nature remains neutral with regard to jurisdictional claims in published maps and institutional affiliations.